Cancer Biol Med 2019. doi: 10.20892/j.issn.2095-3941.2018.0361

ORIGINAL ARTICLE

Simultaneous inhibition of PI3Kα and CDK4/6 synergistically suppresses KRAS-mutated non-small cell lung cancer

Yuxiang Wang[1,2], Xian Li[1], Xueling Liu[1,2], Yi Chen[2,3], Chunhao Yang[4], Cun Tan[4], Bobo Wang[1], Yiming Sun[2,3], Xi Zhang[1], Yinglei Gao[2,3], Jian Ding[2,3], Linghua Meng[1,2]

[1]Division of Anti-Tumor Pharmacology, Shanghai Institute of Materia Medica, Chinese Academy of Sciences, Shanghai 201203, China; [2]University of Chinese Academy of Sciences, Beijing 100049, China; [3]Division of Anti-Tumor Pharmacology, State Key Laboratory of Drug Research, Shanghai Institute of Materia Medica, Chinese Academy of Sciences, Shanghai 201203, China; [4]Department of Medicinal Chemistry, Shanghai Institute of Materia Medica, Chinese Academy of Sciences, Shanghai 200120, China

ABSTRACT

Objective: Activating *KRAS* mutations are the most common drivers in the development of non-small cell lung cancer (NSCLC). However, unsuccess of treatment by direct inhibition of KRAS has been proven. Deregulation of PI3K signaling plays an important role in tumorigenesis and drug resistance in NSCLC. The activity of PI3Kα-selective inhibition against KRAS-mutated NSCLC remains largely unknown.

Methods: Cell proliferation was detected by sulforhodamine B assay. Cell cycle distribution and apoptosis were measured by flow cytometry. Cell signaling was assessed by Western blot and immunohistochemistry. RNA interference was used to down-regulate the expression of cyclin D1. Human NSCLC xenografts were employed to detect therapeutic efficacy *in vivo*.

Results: CYH33 possessed variable activity against a panel of KRAS-mutated NSCLC cell lines. Although CYH33 blocked AKT phosphorylation in all tested cells, Rb phosphorylation decreased in CYH33-sensitive, but not in CYH33-resistant cells, which was consistent with G1 phase arrest in sensitive cells. Combined treatment with the CDK4/6 inhibitor, PD0332991, and CYH33 displayed synergistic activity against the proliferation of both CYH33-sensitive and CYH33-resistant cells, which was accompanied by enhanced G1-phase arrest. Moreover, down-regulation of cyclin D1 sensitized NSCLC cells to CYH33. Reciprocally, CYH33 abrogated the PD0332991-induced up-regulation of cyclin D1 and phosphorylation of AKT in A549 cells. Co-treatment with these two drugs demonstrated synergistic activity against A549 and H23 xenografts, with enhanced inhibition of Rb phosphorylation.

Conclusions: Simultaneous inhibition of PI3Kα and CDK4/6 displayed synergistic activity against KRAS-mutated NSCLC. These data provide a mechanistic rationale for the combination of a PI3Kα inhibitor and a CDK4/6 inhibitor for the treatment of KRAS-mutated NSCLC.

KEYWORDS PI3Kα; CDK4/6; KRAS; NSCLC; CYH33

Introduction

Lung cancer is the most commonly diagnosed cancer and the leading cause of cancer-related deaths[1]. Non-small cell lung cancer (NSCLC) represents over 80% of primary lung cancers. Alterations in *KRAS*, *EGFR* , and *ALK* have been identified as the drivers leading to NSCLC[2,3]. Small molecules targeting tyrosine kinases have been approved to treat NSCLC harboring *EGFR* mutations or *ALK* rearrangements[4]. Unfortunately, molecularly targeting mutated KRAS has remained unsuccessful in the treatment of NSCLC[4]. Mutations in KRAS predominantly arise as substitutions of single amino acids, such as G12, G13, or Q61[5]. These mutations compromise the GTPase activity of KRAS, render constitutive binding with GTP, and lead to ligand-independent, constitutive activation of KRAS. Hyperactive KRAS initiates and maintains activation of intracellular signaling pathways to promote cell proliferation and survival. Furthermore, *KRAS* mutations have been reported to be involved in the development of acquired resistance of NSCLC to EGFR inhibitors[6]. Currently, platinum-based doublet chemotherapy is the standard first-line treatment for KRAS-mutated NSCLC patients. Although the direct inhibition of KRAS is under rigorous investigation, targeting downstream effectors of KRAS has been shown as a potential alternative

Correspondence to: Jian Ding and Linghua Meng
E-mail: jding@simm.ac.cn and lhmeng@simm.ac.cn
Received September 20, 2018; accepted December 25, 2018.
Available at www.cancerbiomed.org

treatment strategy for KRAS-mutated NSCLC. For example, MEK inhibitors, in combination with chemotherapies or targeted drugs, are currently being evaluated in clinical trials.

The PI3K-AKT-mTOR signaling cascade is an important effector downstream of KRAS[7]. Upon activation of receptor tyrosine kinases (RTKs), PI3Kα is activated by either the RTK itself or the intermediates, insulin receptor substrate 1 (IRS-1) and RAS. Activated PI3Kα catalyzes the conversion of phosphatidylinositol-4,5-biphosphate (PIP_2) to phosphatidylinositol-3,4,5-triphosphate (PIP_3) on the inner membrane of the cell, while phosphatase and tensin homolog (PTEN) acts as a negative regulator of the PI3K pathway by converting PIP_3 to PIP_2. PIP_3 leads to full activation of AKT and regulates multiple cellular processes, such as metabolism, proliferation, and apoptosis. Deregulation of the PI3K pathway has been found in 89.4% of NSCLC patients, including alterations in upstream regulators and key components of the pathway, such as *PIK3CA* mutation and amplification, PTEN loss, and AKT aberration[8]. The aberrant PI3K pathway is also involved in the resistance of NSCLC to EGFR inhibitors[9]. Targeting the PI3K pathway has been validated as an important strategy for NSCLC therapy. The PI3Kα-selective inhibitor, BYL719, and the PI3Kβ-sparing inhibitor, GDC-0032, are currently in phase II clinical trials for the treatment of NSCLC (NCT02276027, NCT02785913). PI3Kα is the major isoform that transduces the KRAS signal, but the activity of PI3Kα-selective inhibitors against KRAS-mutated NSCLC remains largely unknown.

CYH33 is a novel PI3Kα-selective inhibitor with a distinctive structure, which was discovered by our group and is currently in clinical trials (NCT03544905). CYH33 displays potent activity against cancers originating from different tissue types, including breast cancer[10]. In this study, we found that CYH33 possessed variable activity against a panel of KRAS-mutated NSCLC cell lines and that decreased Rb phosphorylation was associated with CYH33 efficacy. Consequently, a combination of the CDK4/6 inhibitor, PD0332991, and CYH33 displayed synergistic activity against NSCLC *in vitro* and *in vivo*. This study provides a mechanistic rationale for a combination approach, using a PI3Kα inhibitor and a CDK4/6 inhibitor for the treatment of KRAS-mutated NSCLC.

Materials and methods

Cell lines and culture methods

The human NSCLC cell lines, A549, NCI-H23, NCI-H358, NCI-H460, NCI-H647, NCI-H1355, and NCI-H1792 were purchased from ATCC and authenticated with short tandem repeat (STR) profiling by Genesky Biotechnologies Inc (Shanghai, China). A549 cells were maintained in Ham's F-12 Medium (Corning, NY, USA), and the remaining cell lines were maintained in RPMI 1640 medium (Corning), supplemented with sodium pyruvate (1 mM) and glucose (2500 mg/L). All culture media were supplemented with 10% heat-inactivated fetal bovine serum (FBS).

Compounds

CYH33 was synthesized and provided by Dr. Chunhao Yang (Shanghai Institute of Materia Medica, Chinese Academy of Sciences, Shanghai, China). PD0332991 was purchased from Selleck (Shanghai, China). For *in vitro* experiments, 10 mM stock solutions of CYH33 and PD0332991 were prepared in dimethyl sulfoxide (DMSO; Sigma-Aldrich, St. Louis, MO, USA). For *in vivo* studies, CYH33 was dissolved in normal saline containing 0.5% Tween 80 (v/v; Sangon Biotech, Shanghai, China) and 1% CMC-Na (m/v). PD0332991 was dissolved in sodium lactate (50 mM, pH 4).

Cell proliferation assays

Cell proliferation was measured by a standard sulforhodamine B (SRB, Sigma-Aldrich) assay, as described previously[11].

Flow cytometry

Samples for analysis of cell cycle distribution and apoptosis were prepared as previously described[12,13]. Data were collected with a FACSCalibur Instrument (BD Biosciences, Franklin Lake, NJ, USA) and analyzed with FlowJo software.

Western blot

Cell lysates were collected and subjected to standard Western blot protocols[11] with antibodies against phospho-AKT (Ser473), AKT, phospho-Rb (Ser807/811), phospho-Rb (Ser780), Rb, PARP, caspase 3, caspase 9 (Cell Signaling Technology, Danvers, MA, USA), cyclin D1 (Selleck), and β-actin (Sigma-Aldrich).

SiRNA transfection

SiRNA duplexes were synthesized by GenePharma (Shanghai, China). The sequences of the three siRNAs targeting CCND1 were as follows: 5′-GCAUGUUCGUGGCCUCUAATT-3′, 5′-

CCCGCACGAUUUCAUUGAATT-3′ and 5′-CCACAGAU GUGAAGUUCAUTT-3′. A negative control siRNA was provided by GenePharma, with the following sequence: 5′-UUCUCCGAACGUGUCACGUTT-3′. Cells were grown to 80% confluence in 6-well culture plates and then transfected with CCND1-targeting or negative control siRNAs using Lipofectamine RNAiMAX transfection reagent (Invitrogen, Carlsbad, CA, USA), according to the manufacturer's instructions.

Animal studies

All experiments were performed according to the Institutional Ethical Guidelines on Animal Care and were approved by the Institute of Animal Care and Use Committee at Shanghai Institute of Materia Medica. Four-to-five-week-old female BALB/c athymic nude mice were obtained from the Shanghai Institute of Materia Medica (Shanghai, China). Cells (5×10^6, A549 or H23) suspended in Matrigel were injected subcutaneously into the right side of axillary. When the volume of the xenograft reached 100–200 mm^3, animals were randomized to receive the vehicle control (12 mice per group) or tested compounds (6 mice per group). Vehicle (sodium lactate, 50 mM, pH 4), CYH33 (5 mg/kg), PD0332991 (50 or 100 mg/kg), or a combination of CYH33 and PD0332991 were administered orally for 21 days. Tumor volumes (measured manually with calipers) and body weights were measured twice per week.

Immunohistochemistry

Tumor tissues were harvested and fixed in 4% paraformaldehyde at the end of the animal studies. Tumor tissues were then embedded in paraffin and immunohistochemistry was performed with antibodies against phospho-Rb (Ser780) and Ki67 (Cell Signaling Technology).

Combination analysis

Drug combination studies were performed according to the method of Chou–Talalay[14]. Cells were treated with CYH33 and PD0332991 at a fixed concentration ratio (1:1) for 72 h. The inhibitory rates of the single compound and of the combination of the two compounds were determined by SRB assay. Data were analyzed using Calcusyn software (Biosoft, Cambridge, UK) to determine the combination index (CI) at the GI_{50}. A CI = 1 indicated an additive effect, a CI > 1 indicated antagonism, and a CI < 1 indicated synergism.

The combinatorial effect *in vivo* was evaluated by combination ratio using the fractional product method[15], which is defined as either synergy, additive effect, or antagonism when the combination ratio was > 1, = 1, or < 1, respectively.

Microarray analysis

Total RNA was extracted with TRIzol Reagent (Thermo Fisher, Waltham, MA, USA) and then analyzed on a GeneChip (Affymetrix, Santa Clara, CA, USA) by Shanghai Baygene Biotechnologies Company Limited (Shanghai, China), affiliated to Hong Kong Gene Group Holdings.

Statistical analysis

All data were analyzed using Prism 6 (GraphPad, La Jolla, CA, USA). Data were presented as mean ± SD from at least three independent experiments and differences were considered significant when $P < 0.05$, as determined by Student's *t*-test.

Results

CYH33 induced G1 arrest and suppression of Rb phosphorylation in sensitive KRAS-mutated NSCLC cells

CYH33 is a novel PI3Kα-selective inhibitor displaying potent activity against breast cancer[10]. As PI3Kα is important in mediating signaling downstream of KRAS[16] and mutations in *KRAS* and *PIK3CA* are frequently found in NSCLC[17], we investigated the anti-proliferative activity of CYH33 in a panel of NSCLC cells harboring activating hotspot *KRAS* mutations. Alterations in *EGFR*, *PIK3CA*, *TP53*, and *LKB1* genes found in these cells are depicted in **Figure 1A**. CYH33 significantly inhibited the proliferation of H460, H358, and A549 cells with a $GI_{50} < 1$ μM, while the rest of the cell lines were less responsive to CYH33, with $GI_{50}s > 1$ μM (**Figure 1A**). To investigate the mechanism leading to differential sensitivity to CYH33 in KRAS-mutated NSCLC cells, we detected the level of phosphorylated AKT as a surrogate marker for PI3K activity[18]. As shown in **Figure 1B**, CYH33 decreased phosphorylation of AKT at Ser473 in a dose-dependent manner. CYH33 reduced phosphorylated AKT (pAKT) levels at a concentration of 10 nM in sensitive cells, while higher concentrations were required to achieve similar inhibition in resistant cells. Nevertheless, at a concentration of 100 nM, CYH33 significantly inhibited AKT

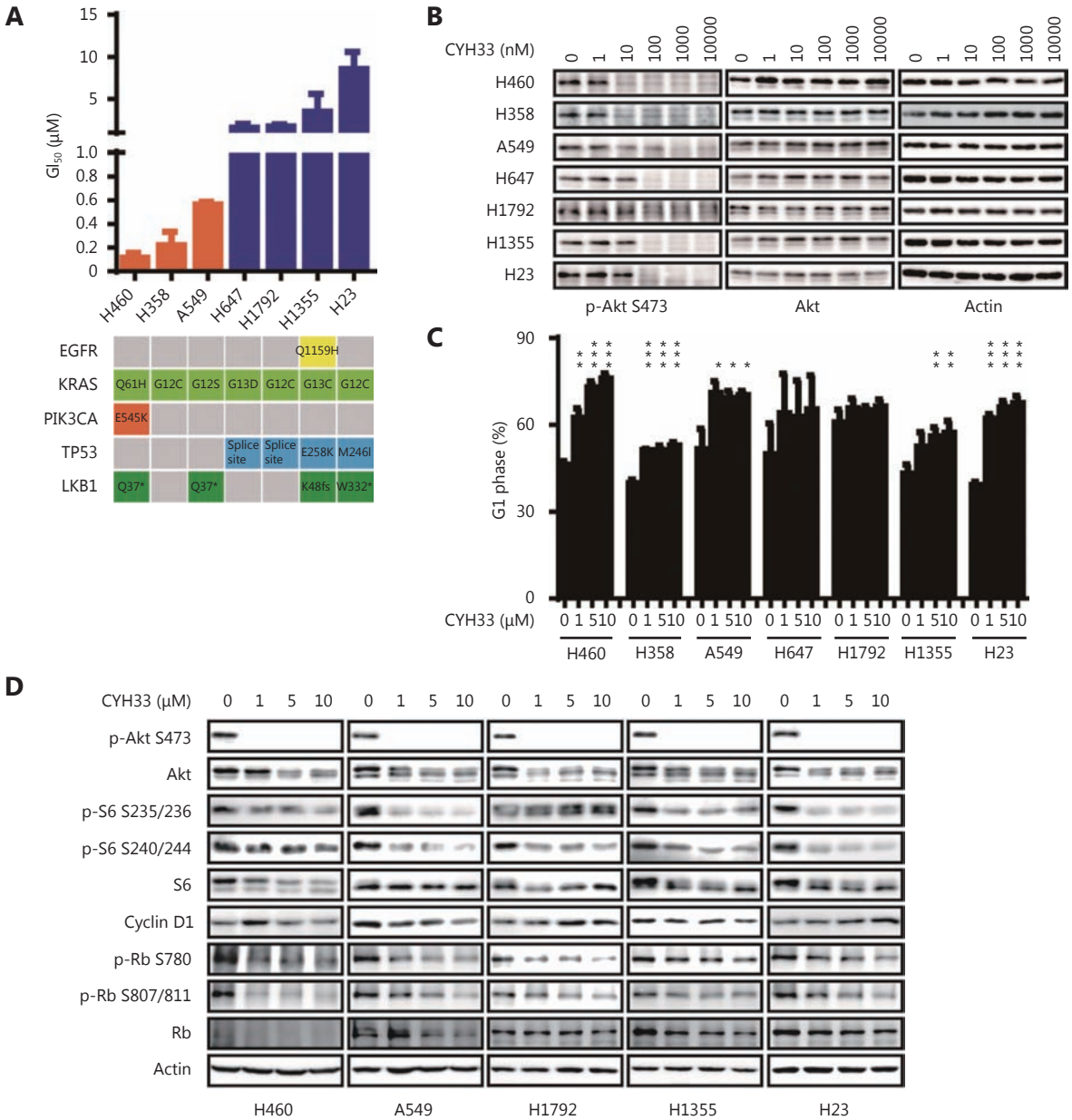

Figure 1 CYH33 induced G1 arrest and suppression of Rb phosphorylation in sensitive KRAS-mutated NSCLC cells. (A) The half-maximal inhibitory concentration against cell growth (GI_{50}) values of CYH33 against the proliferation of seven KRAS-mutated NSCLC cell lines. Bars: mean ± SD. Boxes below the chart indicate mutations in *EGFR*, *KRAS*, *PIK3CA*, *TP53*, or *LKB1*. (B) NSCLC cells were treated with CYH33 at the indicated concentrations for 1 h. Cell lysates were subjected to Western blot with the indicated antibodies. (C) NSCLC cells were treated with CYH33 for 72 h and cell cycle distribution was analyzed by flow cytometry. The cell population in G0/G1 phase is presented as mean + SD. Differences between control (0) and CYH33 treatment groups were analyzed using a two-tailed Student's *t* test. **P* < 0.05; ***P* < 0.01; ****P* < 0.001. (D) Cells were treated with CYH33 at indicated concentrations and cell lysates were subjected to Western blot with indicated antibodies.

phosphorylation in both sensitive and tolerant cells. However, a significantly higher concentration of CYH33 was required to inhibit cell proliferation by 50% in resistant cells.

As PI3K promotes cell cycle progression, which plays critical roles in the initiation and development of tumors, we investigated whether the different sensitivities to CYH33 were due to different effects on cell cycle distribution in KRAS-mutated NSCLC cell lines. As shown in **Figure 1C**, at a

concentration of 1 μM, CYH33 caused a significant arrest of sensitive cells at G1 phase, but it had little effect on the cell population in resistant H647, H1792, and H1355 cells. Unexpectedly, CYH33 treatment resulted in a significant accumulation of H23 cells at G1 phase, which appeared contradictory to its weak activity on the proliferation of H23 cells. We then further investigated the cell cycle progression of A549 and H23 cells. After releases from M phase, H23, but not A549 cells, progressed into S phase in the presence of CYH33 (**Supplementary Figure S1**). This induction of G1 phase arrest by CYH33 seemed to correlate with its anti-proliferative activity. Consistently, a decrease in the levels of phosphorylated Rb was observed in sensitive A549 and H460 cells, but not in resistant H1792, H1355, and H23 cells (**Figure 1D**) after incubation with CYH33 for longer times.

Combined treatment with CYH33 and PD0332991 is synergistic against KRAS-mutated NSCLC cells

The CDK4/6-cyclin D1 complex phosphorylates Rb at G1 phase. This is a vital event for G1/S transition by inducing the expression of downstream regulators that promote cell cycle progression[19]. As Rb phosphorylation was not prevented in CYH33-resistant cells, we hypothesized that inhibition of CDK4/6 would enhance the response of these cells to CYH33. As shown in **Figure 2A**, KRAS-mutated NSCLC cells were treated with increasing doses of CYH33 in combination with the FDA-approved CDK4/6 inhibitor, PD0332991. The inhibitory curve after co-treatment with CYH33 and PD0332991 shifted to the upper left compared to the inhibitory curve after single-agent treatment, indicating an enhanced response in both CYH33-sensitive and CYH33-resistant cells (**Figure 2A**). We further calculated the combination index (CI) using the Chou–Talalay method[14]. As shown in **Figure 2B**, the combination of CYH33 and PD0332991 displayed a synergetic effect (CI < 1) in both resistant and sensitive cells, with the exception of H358 cells, which are very sensitive to CYH33. Moreover, CI values obtained in CYH33-resistant cells were lower than those in CYH33-sensitive cells, indicating more of a synergistic effect in tolerant cells. Accordingly, the GI_{50} values after treatment with CYH33 and PD0332991 were substantially lower than those obtained after treatment with either single agent (**Figure 2C**). To further confirm the synergism between PI3Kα inhibitors and CDK4/6 inhibitors, we tested the combinatorial effect of the PI3Kα inhibitors, CYH33 and BYL719, and the CDK4/6 inhibitors, LEE011 and PD0332991, in H1355 cells. As shown in **Supplementary Figure S2A**, the CI values obtained from the combination of a PI3Kα inhibitor and a CDK4/6 inhibitor were less than 1, indicating synergism between the combinations tested. Moreover, we also tested the combination of PD0332991 and inhibitors targeting the PI3K pathway including, AZD8055, BEZ235, and GDC0941. These combinations also displayed synergistic effects in the tested KRAS-mutated NSCLC cells (**Supplementary Figure S2B**). Thus, simultaneously targeting PI3K and CDK4/6 showed synergistic activity against KRAS-mutated NSCLC cells.

Combined CYH33 and PD0332991 treatment induces significant G1 phase arrest in KRAS-mutated NSCLC cells

PD0332991 inhibits the activity of CDK4/6, which phosphorylates Rb and promotes G1/S progression. PI3K also regulates G1/S progression through the inhibition of cyclin D1 proteolysis and inactivation of p27[20,21]. We next investigated whether the synergism between CYH33 and PD0332991 was due to their combined effect on cell cycle distribution. As shown in **Figure 3A**, combined treatment significantly increased the cell population in G1 phase compared to treatment with either single agent, in both sensitive and tolerant cells. Further dissection of the signaling pathway showed that CYH33 inhibited Rb phosphorylation in sensitive H460 and A549 cells, but not in resistant H1355 and H23 cells (**Figure 3B**). PD0332991 alone suppressed Rb phosphorylation in all cell lines. Co-treatment with CYH33 and PD0332991 blocked Rb phosphorylation to a greater extent than single-agent treatment (**Figure 3B**), which was consistent with the increase in G1 phase arrest.

Long-term cell cycle arrest can induce apoptosis. To examine whether the enhanced response of KRAS-mutated NSCLC cells to the combination of CYH33 and PD0332991 was due to the induction of apoptosis, annexin V staining was performed after A549 and H23 cells were treated for 72 h. As shown in **Figure 3C** and **3D**, annexin V-positive cells slightly increased in the presence of CYH33 and supplementation with PD0332991 failed to further increase this cell population. Similar results were obtained with the other five KRAS-mutated NSCLC cell lines (**Supplementary Figure S3**). Consistently, no cleaved PARP or caspase 3/9 were detected in A549 and H23 cells treated with CYH33 and PD0332991 alone or in combination (**Figure 3E**). Thus, combined treatment with CYH33 and PD0332991 inhibited the proliferation of KRAS-mutated NSCLC cells by inducing G1 phase arrest rather than inducing apoptosis.

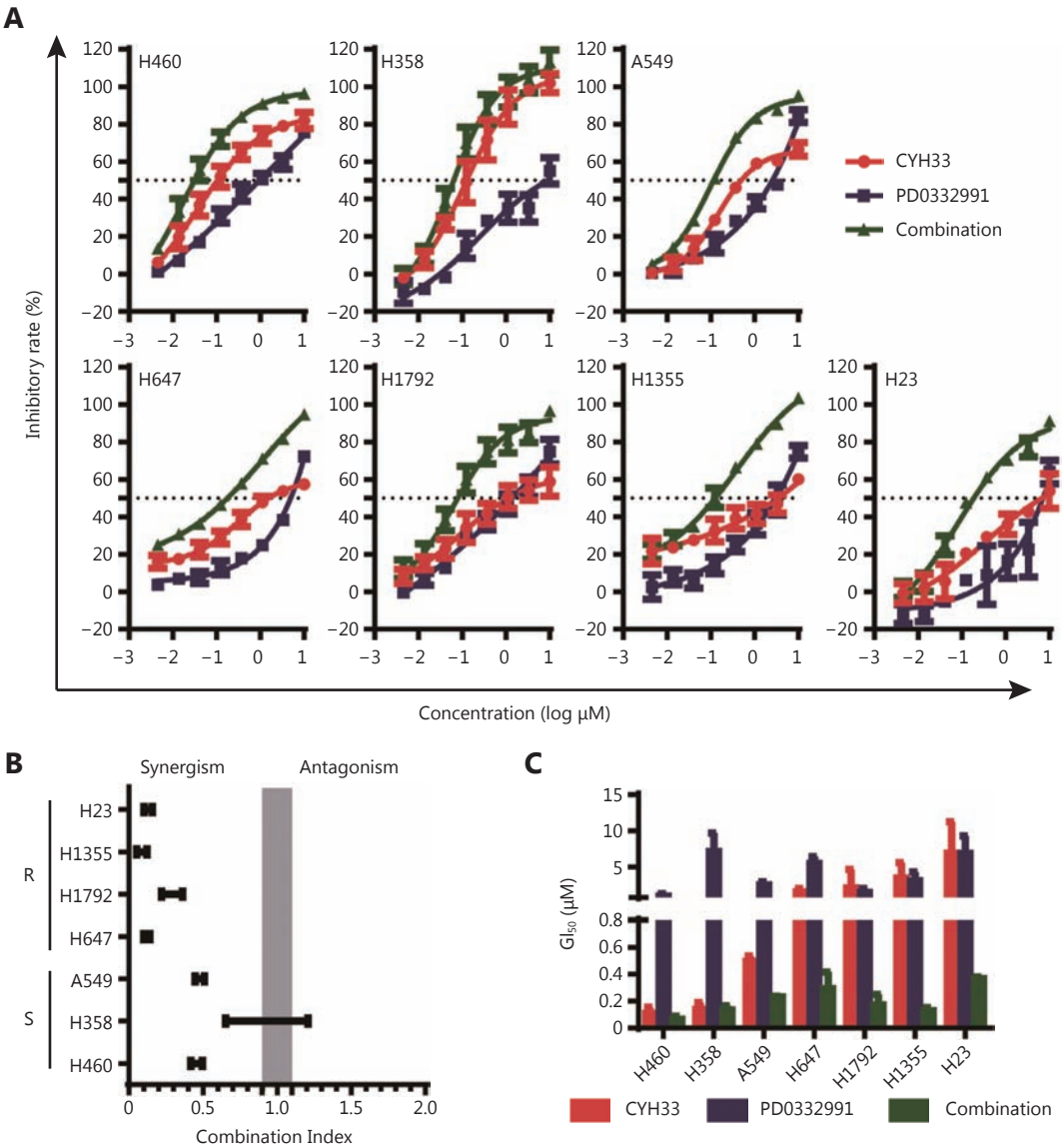

Figure 2 Combined treatment of CYH33 and PD0332991 is synergistic against KRAS-mutated NSCLC cells. KRAS-mutated NSCLC cells were treated with CYH33, PD0332991, or both CYH33 and PD0332991 for 72 h and cell proliferation was detected by SRB assay. (A) Inhibitory curves from three independent experiments are presented. (B) CI values at the GI_{50} of seven NSCLC cancer cell lines were determined by the Chou-Talalay method. Gray bar: CI values indicating additive effect. R: CYH33-resistant cell lines; S: CYH33-sensitive cell lines. (C) GI_{50} values for CYH33, PD0332991, or the combination of CYH33 and PD03329917 against KRAS-mutated NSCLC cells. Data are shown as mean ± SD.

Down-regulation of cyclin D1 sensitizes KRAS-mutated NSCLC cells to CYH33

To confirm that the inhibition of CDK4/6 sensitized NSCLC cells to CYH33, we down-regulated the expression of cyclin D1, which is an essential factor for the kinase activity of CDK4 and CDK6. As shown in **Figure 4A** and **4B**, knocking down cyclin D1 expression using specific siRNAs rendered A549 (**Figure 4A**) and H23 (**Figure 4B**) cells more sensitive to CYH33. Transfection of siRNAs targeting cyclin D1 also resulted in enhanced cell cycle arrest at G1 phase upon CYH33 treatment compared to cells transfected with scrambled siRNA (NC, **Figure 4C** and **4D**). In agreement with these observations, down-regulation of cyclin D1 further reduced the level of phosphorylated Rb in the presence of CYH33 (**Figure 4E** and **4F**). Knocking down cyclin D1 failed to

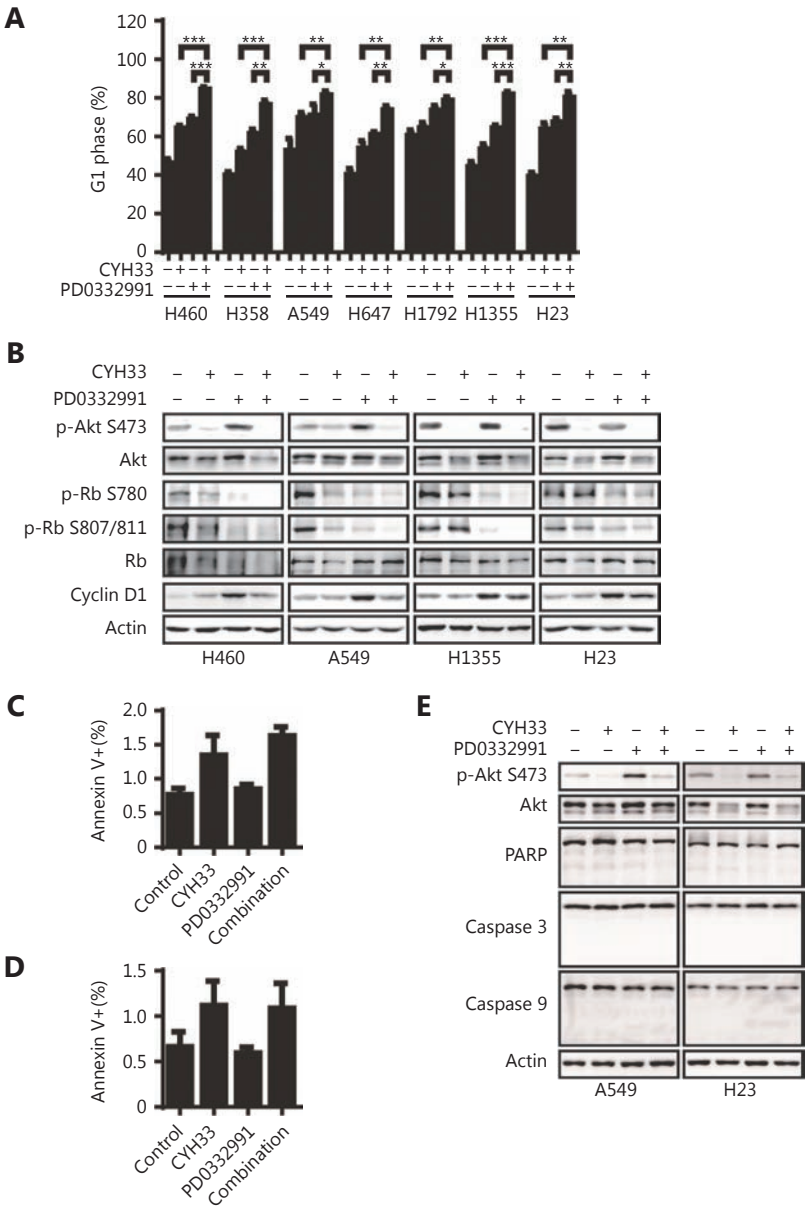

Figure 3 Combined CYH33 and PD0332991 treatment induces significant G1 phase arrest in KRAS-mutated NSCLC cells. KRAS-mutated NSCLC cells were treated with vehicle, CYH33 (1 μM), PD0332991 (1 μM), or both CYH33 and PD0332991 for 72 h. (A) Cell cycle distribution was analyzed by flow cytometry. The cell population in G0/G1 phase is presented as the mean ± SD. Differences between the indicated groups were analyzed using a two-tailed Student's *t* test. **P* < 0.05; ***P* < 0.01; ****P* < 0.001. (B) Cell lysates were subjected to Western blot with the indicated antibodies. Induction of apoptosis of A549 (C) and H23 (D) cells was determined by annexin-V-PI dual staining. Annexin-V positive cells were determined with flow cytometry. Data are shown as the mean ± SD from three independent experiments. (E) Lysates of A549 and H23 cells were subjected to Western blot with the indicated antibodies.

enhance the ability of CYH33 to induce apoptosis (**Supplementary Figure S4A-D**), which is consistent with the results obtained with co-treatment of CYH33 and PD0332991. However, down-regulation of cyclin D1 failed to enhance the anti-proliferative activity of PD0332991 in A549 and H23 cells (**Supplementary Figure S4E** and **S4F**), which might be due to the similar cellular targets of PD0332991 and the siRNAs. Thus, down-regulation of cyclin D1 using siRNAs mimicked the function of PD0332991 in combination with CYH33, suggesting that the synergistic effect of CYH33 and

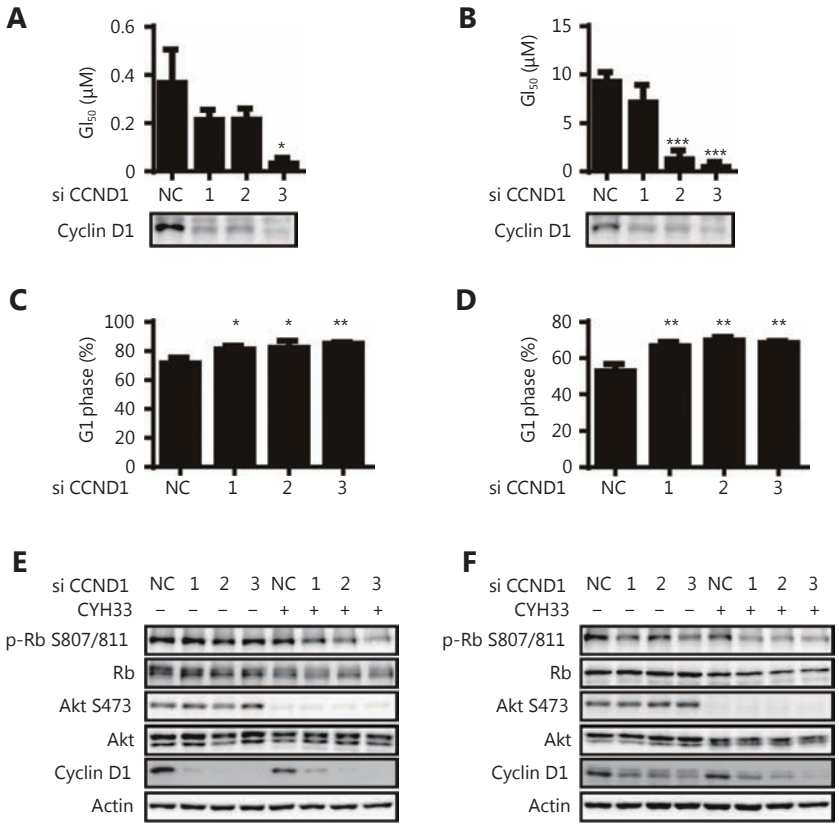

Figure 4 Down-regulation of cyclin D1 sensitizes A549 and H23 cells to CYH33. A549 and H23 cells transfected with siRNAs targeting cyclin D1 or a negative control (NC) siRNA were treated with serially diluted CYH33 (A, B) or CYH33 at 1 μM for 72 h (C, F). (A, B) The effect of CYH33 on cell proliferation was determined by SRB assay. GI_{50} values obtained from A549 (A) and H23 (B) cells are presented. (C, D) The cell cycle distribution of A549 (C) and H23 (D) cells was analyzed by flow cytometry. The cell population in G0/G1 phase is presented. (E, F) Lysates of A549 (E) and H23 (F) cells were subjected to Western blot with the indicated antibodies. Data are shown as the mean + SD or representatives from at least three independent experiments. Differences between cells transfected with an NC siRNA and siRNAs targeting cyclin D1 were analyzed using a two-tailed Student's *t* test. **P* < 0.05; ***P* < 0.01; ****P* < 0.001.

PD0332991 was due to a more complete inhibition of Rb phosphorylation and in turn, G1 phase arrest.

CYH33 abrogates PD0332991-induced AKT phosphorylation and cyclin D1 expression

It has been reported that inhibition of CDK4/6 results in the feed-back expression of cyclin D1 in breast cancer[22], which would impede the activity of CDK4/6 inhibitors in the treatment of breast cancer. To further explore the mechanism underlying the synergy between PD0332991 and CYH33, we performed microarray analysis in A549 cells treated with 1 μM PD0332991 or vehicle for 72 h (**Supplementary Figure S5A**). As expected, the "E2F target" hallmark gene set was among the top enriched gene sets (**Figure 5A**) that were down-regulated after PD0332991 treatment. Cell cycle-associated processes, like "G2M checkpoint" and "mitotic spindle" (**Supplementary Figure S5B**) were also down-regulated due to PD0332991-induced G1 phase cell cycle arrest. Meanwhile, PI3K signaling tended to be activated after PD0332991 treatment (**Figure 5B**) and was accompanied by the up-regulation of growth factors, like insulin (*INS*), insulin like growth factor 1 (*IGF1*), and cyclin D1 (*CCND1*). However, the expression of PTEN, which acts as an important negative regulator of PI3K, was down-regulated after PD0332991 treatment (**Figure 5B**). Accordingly, PD0332991 slightly increased AKT phosphorylation, but significantly induced the expression of cyclin D1 (**Figure 5C**). Furthermore, CYH33 abrogated PD0332991-induced AKT phosphorylation and cyclin D1 expression (**Figure 5D**), which may also contribute the synergistic activity of CYH33 and PD0332991.

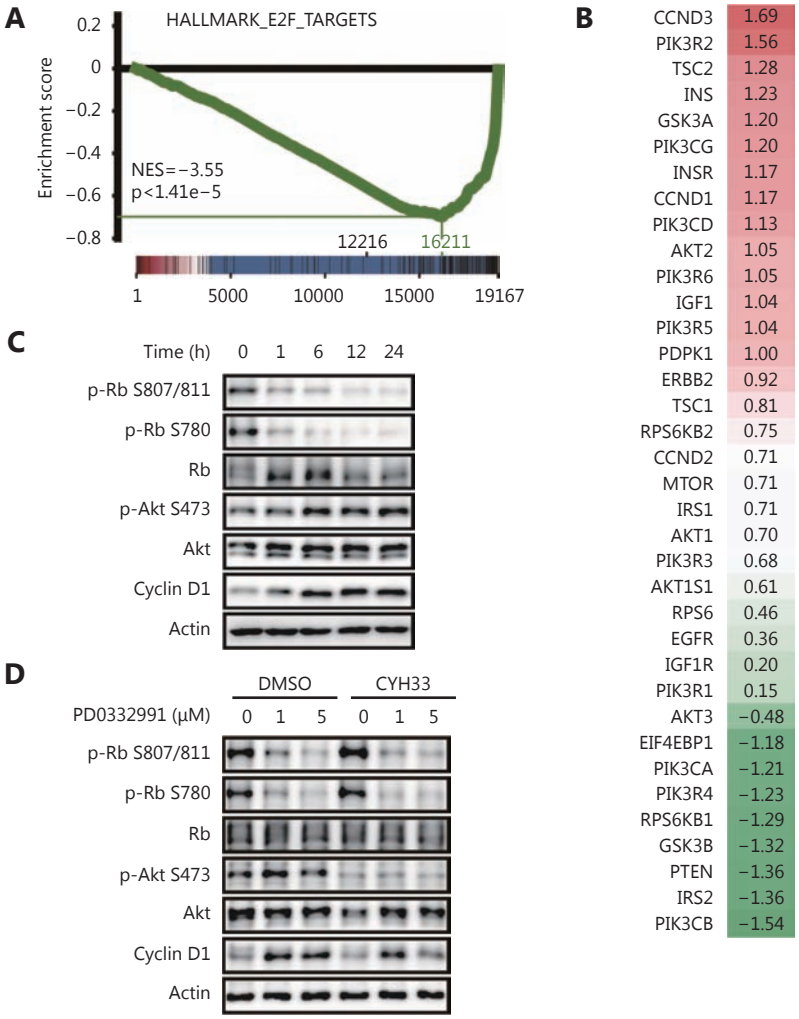

Figure 5 CYH33 abrogates PD0332991-induced AKT phosphorylation and cyclin D1 expression. (A, B) A549 cells were treated with vehicle or PD0332991 (1 μM) for 72 h and total RNA were extracted. Genome-wide gene expression profiling was performed by microarray analysis. (A) GSEA enrichment plot of differentially expressed genes in the gene set of Hallmark of E2F targets (HALLMARK_E2F_TARGETS) after treatment with PD0332991. (B) Heatmap of the mRNA levels of genes involved in the PI3K-AKT signaling pathway. The fold change (log 2) in the expression of the listed genes after treatment with 1 μM PD0332991 is shown. (C) A549 cells were treated with 1 μM PD0332991 for the indicated times and cell lysates were subjected to Western blot with the indicated antibodies. (D) A549 cells were treated with PD0332991 (0, 1 or 5 μM) alone or in combination with CYH33 (1 μM) for 72 h and cell lysates were subjected to Western blot with the indicated antibodies. Data are shown as representatives from at least three independent experiments.

Combined inhibition of PI3Kα and CDK4/6 displays synergistic activity against KRAS-mutated NSCLC xenografts

Combined treatment with CYH33 and PD0332991 was shown to be synergetic against a panel of KRAS-mutated NSCLC cells. We next examined the efficacy of CYH33 and PD0332991 in A549 and H23 xenografts. After treatment for 21 d, PD0332991 treatment at 50 mg/kg marginally suppressed the growth of A549 xenografts, yielding a treated/control (T/C) value of 76.9 %, whereas CYH33 treatment at 5 mg/kg displayed potent activity, with a T/C value of 49.2%. Co-administration of CYH33 and PD0332991 significantly enhanced the potency compared to single-agent treatment, with a T/C value of 26.1% (**Figure 6A**, **Supplementary Figure S6A**). Similar results were also obtained with H23 xenografts (**Figure 6B**, **Supplementary Figure S6A**). We did not observe a significant loss in body weight in treated animals (**Figure 6A** and **6B**), indicating a favorable safety profile of the combined treatment. We then

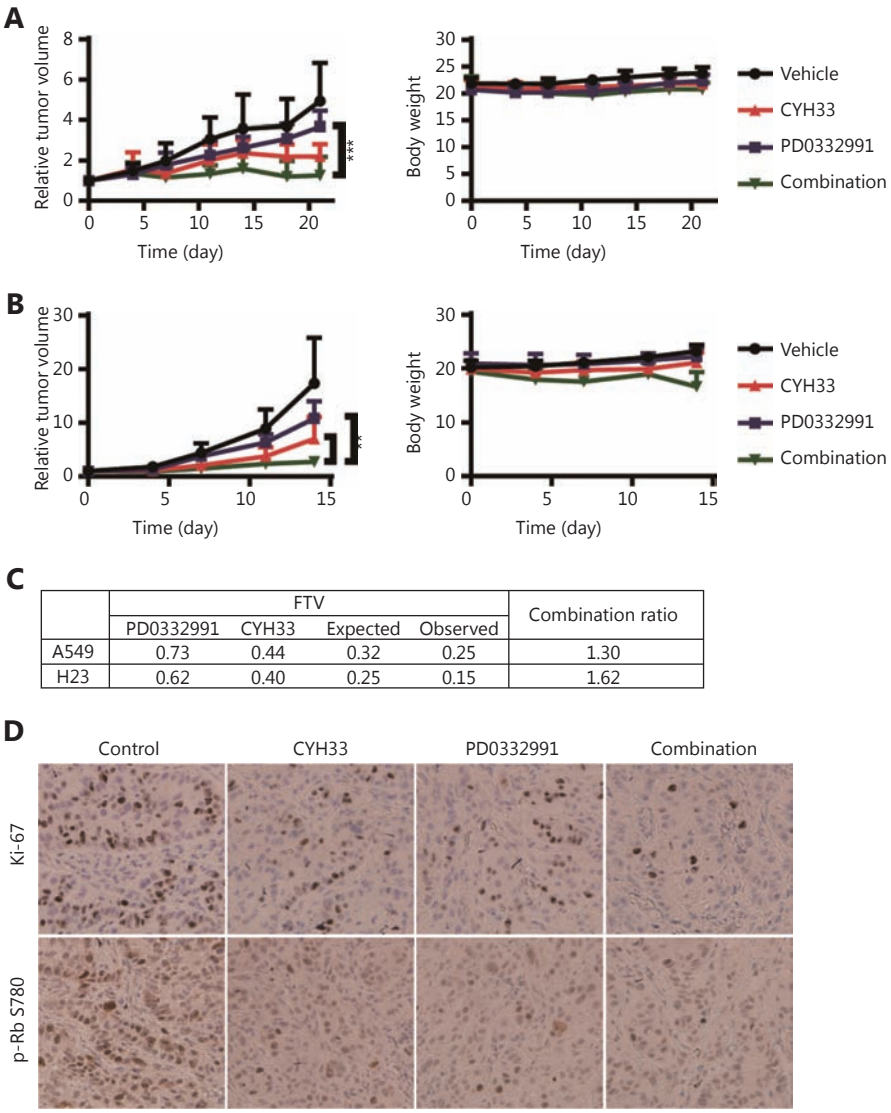

	FTV				Combination ratio
	PD0332991	CYH33	Expected	Observed	
A549	0.73	0.44	0.32	0.25	1.30
H23	0.62	0.40	0.25	0.15	1.62

Figure 6 Combined inhibition of PI3Kα and CDK4/6 displays synergistic activity against A549 and H23 xenografts. Randomly grouped nude mice bearing A549 (A) or H23 (B) xenografts were administrated orally with a vehicle control, CYH33 (5 mg/kg), PD0332991 (50 mg/kg for mice bearing A549 xenografts, 100 mg/kg for mice bearing H23 xenografts), or a combination of CYH33 and PD0332991, once a day for the indicated times. Tumor volume and body weight were measured twice a week. Data are depicted as the mean + SD (n = 6). Differences between the indicated groups were analyzed by Student's t test. *P < 0.05; **P < 0.01; ***P < 0.001. (C) The combination ratios of CYH33 and PD0332991 against A549 and H23 xenografts were calculated using the fractional product method. FTV (fractional tumor volume) = mean final tumor volume of treated group/mean final tumor volume of control group. Expected FTV = (FTV of PD0332991) * (FTV of CYH33). Observed FTV = mean final tumor volume of combinatorial treatment/mean final tumor volume of control group. Combination ratio = expected FTV/observed FTV. (D) Tumor sections from A549 xenografts after treatment for 21 d were stained with Ki-67 (tawny) or phosphorylated Rb (Ser780, tawny). Cell nuclei were stained with hematoxylin (calamine blue, 40 ×). Representative images are shown for each group.

calculated the combination ratio of CYH33 and PD0332991, using the fractional product method[15]. The combinatorial effect was defined as synergistic, additive, or antagonistic when the combination ratio was > 1, = 1, or < 1, respectively. The combination ratio of CYH33 and PD0332991 in A549 and H23 xenografts was 1.30 and 1.62, respectively, demonstrating that the combination of CYH33 and PD0332991 displayed synergistic activity to inhibit the

growth of A549 and H23 xenografts (**Figure 6C**). This result is consistent with less Ki67 staining in tumor sections from the combinatorial treatment group compared with tumor sections from groups treated with a single agent (**Figure 6D**). Combined treatment with CYH33 and PD0332991 resulted in enhanced inhibition of Rb phosphorylation at Ser780 *in vivo* (**Figure 6D**), further confirming that the synergy was attributed to augmented inhibition of cell cycle progression. Taken together, combined treatment with CYH33 and PD0332991 reduced Rb phosphorylation and synergistically inhibited the growth of KRAS-mutated NSCLC *in vivo*.

Discussion

Oncogenic mutations in KRAS are prevalent in NSCLC and represent a largely unmet clinical need. In this study, we found that a novel PI3Kα-specific inhibitor, CYH33, possessed variable activity against a panel of KRAS-mutated NSCLC cell lines. Phosphorylated Rb levels were shown to decrease in CYH33-sensitive, but not CYH33-resistant cells, which was consistent with G1 phase arrest in CYH33-sensitive cells. Combination of the CDK4/6 inhibitor, PD0332991, with CYH33 displayed synergistic activity against NSCLS *in vitro* and *in vivo*, which was accompanied by enhanced inhibition of Rb phosphorylation.

The $PIK3CA^{H1047R}$ mutant has been reported to accelerate and enhance the onset of lung cancer initiated by $KRAS^{G12D}$[23] and the *PIK3CA* gene is frequently mutated (3.1%) and/or amplified (17.1%) in NSCLC[23,24]. Indeed, we demonstrated that CYH33 potently inhibited the proliferation of KRAS-mutated NSCLC cells *in vitro* and *in vivo*, confirming that PI3Kα is a promising target for the treatment of NSCLC. It is notable that the response of KRAS-mutated NSCLC cell lines to CYH33 was variable, which may be due to the high genome heterogeneity of tested cell lines. Mutation in *PIK3CA* did not predict the efficacy of CYH33, as H358 and A549 cells expressing wild-type *PIK3CA* were sensitive to CYH33. We dissected the signaling downstream of PI3K and found that a decrease in phosphorylated Rb, rather than phosphorylated AKT, may predict the activity of CYH33 in KRAS-mutated NSCLC. This is in agreement with the observation that mutated PI3Kα cooperated with KRAS in lung tumorigenesis by regulating multiple components of the G1/S transition, including Rb. Consistently, CYH33 induced G1 phase arrest in sensitive, but not in resistant, KRAS-mutated NSCLC cells. A phase II study investigating the pan-PI3K inhibitor, buparlisib (BKM120), in patients with PI3K pathway-activated, relapsed NSCLC, failed to meet its primary objective[25]. Our study indicated that an intermediate response downstream of PI3K might better predict the efficacy of PI3K inhibitors. Moreover, the CDK4/6 inhibitor, PD0332991, sensitized KRAS-mutated NSCLC cells to CYH33, which was accompanied by an enhanced inhibition of Rb phosphorylation and G1 phase arrest. Thus, CYH33 is active against KRAS-mutated NSCLC and a decrease in phosphorylated Rb may predict its efficacy.

We demonstrated that targeting PI3Kα is a potential therapeutic strategy for KRAS-mutated NSCLC. BYL719, the most advanced PI3Kα-selective inhibitor, is in a multiple-arm phase II study of advanced NSCLC (NCT02276027). However, CYH33 is active in part of the tested cell lines. *PIK3CA* mutation is unlikely to be the genetic driver in lung tumorigenesis, as it has been reported to be unable to promote tumor formation[23]. We found that simultaneous inhibition of PI3Kα and CDK4/6 synergistically suppressed the proliferation of KRAS-mutated NSCLC both *in vitro* and *in vivo*. The rationale for the combination of CYH33 and a CDK4/6 inhibitor is based on the discrepancy of CYH33 in the regulation of Rb phosphorylation and cell cycle arrest. Combined inhibition of CDK4/6 and PI3K has been reported to induce synergistic anti-tumor effects in breast cancer and malignant pleural mesothelioma (MPM)[22,26-28], indicating that this combination therapy is a potential strategy to treat cancers with aberrant PI3K or Rb pathways. Although different types of PI3K inhibitors, e.g., PI3K/mTOR dual inhibitor, pan-PI3K, and isoform-selective inhibitors, have been studied in different types of cancers, the synergism is always accompanied by an enhanced inhibition of Rb phosphorylation[26,28], which is consistent with our observation with a novel PI3Kα-selective inhibitor CYH33 in KRAS-mutated NSCLC. Using microarray profiling, we also found that CDK4/6 inhibition resulted in the up-regulation of multiple components of the PI3K pathway. Consequently, CDK4/6 inhibition increased the phosphorylation of AKT and the expression of cyclin D1. PIP_3-dependent protein kinase 1 (PDK1) was identified as a key factor in determining the activity of CDK4/6 inhibitors against breast cancer cells in a kinome-wide siRNA screen[22]. Given that PDK1 is a kinase that directly activates AKT, up-regulation of AKT phosphorylation has been found in breast cancer cells[22], MPM cells[27], and in this study, KRAS-mutated NSCLC cells, after inhibition of CDK4/6. Phosphorylation of AKT and induction of cyclin D1 have been reported to render cancer cells resistant to CDK4/6 inhibitors[22], which provides an additional rationale for using a combination of PI3K and CDK4/6 inhibitors. Indeed, CYH33 abrogated the enhanced phosphorylation of AKT and expression of cyclin D1 in NSCLC cells.

In summary, the combination of CYH33 and PD0332991 demonstrated synergistic activity against a panel of KRAS-mutated NSCLC cells *in vitro* and *in vivo*, which was associated with increased cell cycle arrest at G1 phase. Our findings provide a mechanistic rationale to test CYH33 and other PI3K inhibitors in combination with CDK4/6 inhibitors for treating KRAS-mutated NSCLC in future clinical trials.

Acknowledgements

This work was supported by grants from "Personalized Medicines-Molecular Signature-based Drug Discovery and Development", Strategic Priority Research Program of the Chinese Academy of Sciences (Grant No. XDA12020218 & XDA12020111), National Science and Technology Major Project "Key New Drug Creation and Manufacturing Program" (Grant No. 2018ZX09711002-011-014), and National Natural Science Foundation of China (Grant No. 81773760). This work was partially supported by Fudan-SIMM Joint Research Program (Grant No. FU-SIMM20172005).

Conflict of interest statement

No potential conflicts of interest are disclosed.

References

1. Torre LA, Bray F, Siegel RL, Ferlay J, Lortet-Tieulent J, Jemal A. Global cancer statistics, 2012. Ca-Cancer J Clin. 2015; 65: 87-108.
2. Gainor JF, Varghese AM, Ou SHI, Kabraji S, Awad MM, Katayama R, et al. *ALK* rearrangements are mutually exclusive with mutations in *EGFR* or *KRAS*: An analysis of 1,683 patients with non-small cell lung cancer. Clin Cancer Res. 2013; 19: 4273-81.
3. Zheng DF, Wang R, Ye T, Yu S, Hu HC, Shen XX, et al. MET exon 14 skipping defines a unique molecular class of non-small cell lung cancer. Oncotarget. 2016; 7: 41691-702.
4. Shea M, Costa DB, Rangachari D. Management of advanced non-small cell lung cancers with known mutations or rearrangements: Latest evidence and treatment approaches. Ther Adv Respir Dis. 2016; 10: 113-29.
5. Roberts PJ, Stinchcombe TE. *KRAS* mutation: Should we test for it, and does it matter? J Clin Oncol. 2013; 31: 1112-21.
6. Del Re M, Tiseo M, Bordi P, D'Incecco A, Camerini A, Petrini I, et al. Contribution of *KRAS* mutations and c.2369c > t (p.T790m) *EGFR* to acquired resistance to EGFR-TKIs in *EGFR* mutant NSCLC: A study on circulating tumor DNA. Oncotarget. 2017; 8: 13611-9.
7. Eser S, Schnieke A, Schneider G, Saur D. Oncogenic KRAS signalling in pancreatic cancer. Br J Cancer. 2014; 111: 817-22.
8. Stjernström A, Karlsson C, Fernandez OJ, Söderkvist P, Karlsson MG, Thunell LK. Alterations of INPP4B, PIK3CA and pAkt of the PI3K pathway are associated with squamous cell carcinoma of the lung. Cancer Med. 2014; 3: 337-48.
9. Engelman JA, Mukohara T, Zejnullahu K, Lifshits E, Borrás AM, Gale CM, et al. Allelic dilution obscures detection of a biologically significant resistance mutation in *EGFR*-amplified lung cancer. J Clin Invest. 2006; 116: 2695-706.
10. Liu XL, Xu YC, Wang YX, Chen Y, Wang BB, Wang Y, et al. Decrease in phosphorylated ERK indicates the therapeutic efficacy of a clinical PI3Kα-selective inhibitor CYH33 in breast cancer. Cancer Lett. 2018; 433: 273-82.
11. Shi JJ, Chen SM, Guo CL, Li YX, Ding J, Meng LH. The mTOR inhibitor AZD8055 overcomes tamoxifen resistance in breast cancer cells by down-regulating HSPB8. Acta Pharmacol Sin. 2018; 39: 1338-46.
12. Li X, Tong LJ, Ding J, Meng LH. Systematic combination screening reveals synergism between rapamycin and sunitinib against human lung cancer. Cancer Lett. 2014; 342: 159-66.
13. Liu YX, Qing LH, Meng CS, Shi JJ, Yang Y, Wang ZW, et al. 6-oh-phenanthroquinolizidine alkaloid and its derivatives exert potent anticancer activity by delaying s phase progression. J Med Chem. 2017; 60: 2764-79.
14. Chou TC. Drug combination studies and their synergy quantification using the chou-talalay method. Cancer Res. 2010; 70: 440-6.
15. Watanabe T, Naito M, Kokubu N, Tsuruo T. Regression of established tumors expressing p-glycoprotein by combinations of adriamycin, cyclosporin derivatives, and MRK-16 antibodies. J Natl Cancer Inst. 1997; 89: 512-8.
16. Repasky GA, Chenette EJ, Der CJ. Renewing the conspiracy theory debate: Does raf function alone to mediate ras oncogenesis? Trends Cell Biol. 2004; 14: 639-47.
17. Barlesi F, Mazieres J, Merlio JP, Debieuvre D, Mosser J, Lena H, et al. Routine molecular profiling of patients with advanced non-small-cell lung cancer: Results of a 1-year nationwide programme of the French Cooperative Thoracic Intergroup (IFCT). Lancet. 2016; 387: 1415-26.
18. Elkabets M, Vora S, Juric D, Morse N, Mino-Kenudson M, Muranen T, et al. mTORC1 inhibition is required for sensitivity to PI3K p110α inhibitors in *PIK3CA*-mutant breast cancer. Sci Transl Med. 2013; 5: 196ra99.
19. Kato J, Matsushime H, Hiebert SW, Ewen ME, Sherr CJ. Direct binding of cyclin D to the retinoblastoma gene product (pRb) and pRb phosphorylation by the cyclin D-dependent kinase CDK4. Genes Dev. 1993; 7: 331-42.
20. Majeed R, Hussain A, Sangwan PL, Chinthakindi PK, Khan I, Sharma PR, et al. PI3K target based novel cyano derivative of betulinic acid induces its signalling inhibition by down-regulation of pGSK3β and cyclin D1 and potentially checks cancer cell proliferation. Mol Carcinog. 2016; 55: 964-76.
21. Nölting S, Rentsch J, Freitag H, Detjen K, Briest F, Möbs M, et al. The selective PI3Kα inhibitor BYL719 as a novel therapeutic option

for neuroendocrine tumors: Results from multiple cell line models. PLoS One. 2017; 12: e0182852.

22. Jansen VM, Bhola NE, Bauer JA, Formisano L, Lee KM, Hutchinson KE, et al. Kinome-wide RNA interference screen reveals a role for PDK1 in acquired resistance to CDK4/6 inhibition in ER-positive breast cancer. Cancer Res. 2017; 77: 2488-99.
23. Green S, Trejo CL, McMahon M. PIK3CA^{H1047R} accelerates and enhances KRAS^{G12D}-driven lung tumorigenesis. Cancer Res. 2015; 75: 5378-91.
24. Yamamoto H, Shigematsu H, Nomura M, Lockwood WW, Sato M, Okumura N, et al. *PIK3CA* mutations and copy number gains in human lung cancers. Cancer Res. 2008; 68: 6913-21.
25. Vansteenkiste JF, Canon JL, De Braud F, Grossi F, De Pas T, Gray JE, et al. Safety and efficacy of buparlisib (BKM120) in patients with PI3K pathway-activated non-small cell lung cancer: Results from the phase II BASALT-1 study. J Thorac Oncol. 2015; 10: 1319-27.
26. Vora SR, Juric D, Kim N, Mino-Kenudson M, Huynh T, Costa C, et al. CDK 4/6 inhibitors sensitize *PIK3CA* mutant breast cancer to PI3K inhibitors. Cancer Cell. 2014; 26: 136-49.
27. Bonelli MA, Digiacomo G, Fumarola C, Alfieri R, Quaini F, Falco A, et al. Combined inhibition of CDK4/6 and PI3K/AKT/mTOR pathways induces a synergistic anti-tumor effect in malignant pleural mesothelioma cells. Neoplasia. 2017; 19: 637-48.
28. Shi RS, Li M, Raghavan V, Tam S, Cabanero M, Pham NA, et al. Targeting the CDK4/6-RB pathway enhances response to PI3K inhibition in *PIK3CA*-mutant lung squamous cell carcinoma. Clin Cancer Res. 2018; 24: 5990-6000.

Cite this article as: Wang Y, Li X, Liu X, Chen Y, Yang C, Tan C, et al. Simultaneous inhibition of PI3Kα and CDK4/6 synergistically suppresses KRAS-mutated non-small cell lung cancer. Cancer Biol Med. 2019; 16: 66-78. doi: 10.20892/j.issn.2095-3941.2018.0361

Supplementary materials

Materials and methods

Compound

Nocodazole, BYL719, LEE011, AZD8055, BEZ235 and GDC0941 were purchased from Selleck (Shanghai, China) and stock solution (10 mM) was prepared in dimethyl sulfoxide (DMSO, Sigma-Aldrich, St. Louis, MO, USA).

Cell cycle synchronization and release

A549 and H23 cells were synchronized at G2/M phase by incubation with 0.3 μM nocodazole for 24 h. The medium was replaced with fresh medium to release the progression of cell cycle.

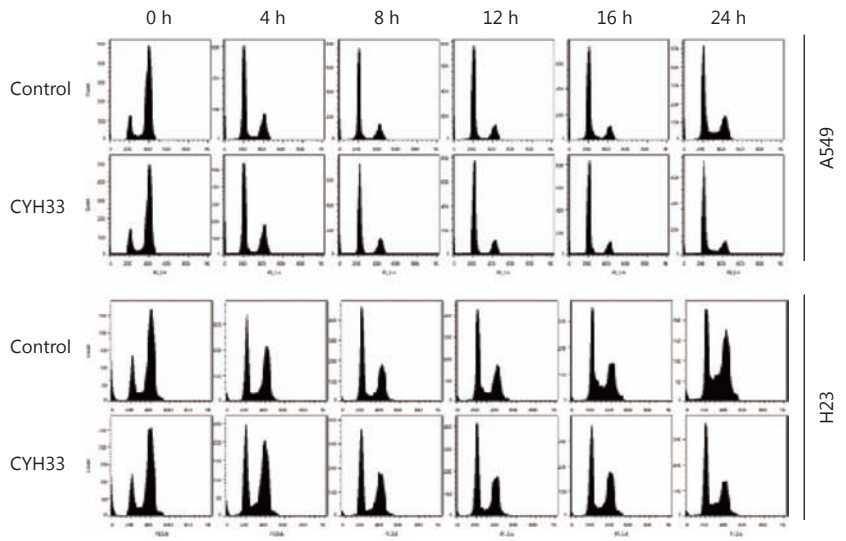

Figure S1 H23 cells progressed into S phase in the presence of CYH33. A549 and H23 cells were synchronized at G2/M phase by incubation with nocodazole (0.3 μM) for 24 h. Cells were further incubated in fresh medium in the absence or presence of CYH33 (1 μM) for indicated times and cell cycle distribution was analyzed with flow cytometry.

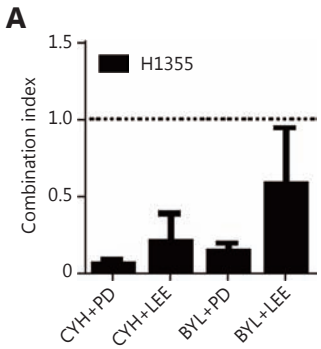

B

Combination index	A549	H460	H358	H23
AZD8055	0.44	0.29	0.47	0.49
BEZ235	0.67	0.57	0.63	0.72
GDC0941	0.28	0.15	0.24	0.35

Figure S2 Co-treatment with PI3K pathway inhibitor and CDK4/6 inhibitor synergistically suppress proliferation of Kras-mutated NSCLC cells. Combination Index (CI) values at GI_{50} of Kras-mutated NSCLC cell lines were determined by Chou-Talalay method. Cell proliferation was detected by SRB assay after cells were treated with each single agent or indicated combination. (A) CI values of PI3Kα inhibitor CYH33 or BYL719 and CDK4/6 inhibitor PD0332991 or LEE011 in H1355 cells. CYH: CYH33, BYL: BYL719, PD: PD0332991, LEE: LEE011. Data shown are the mean + SD. (B) CI values of PD0332991 and PI3K pathway inhibitor AZD8055, BEZ235 or GDC0941 in Kras-mutated NSCLC A549, H460, H358 and H23 cells. Data shown are the mean.

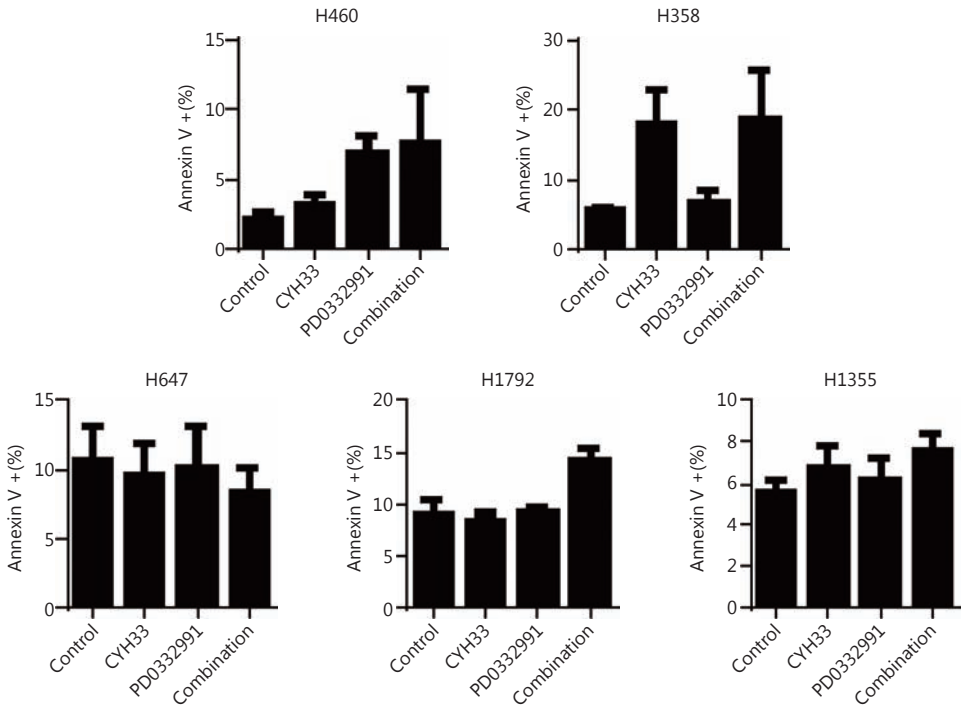

Figure S3 Co-treatment with CYH33 and PD0332991 failed to induce apoptosis in NSCLC cells. Kras-mutated NSCLC cells were treated with CYH33 (1 μM), PD0332991 (1 μM), or both for 72 h and apoptosis was determined by Annexin-V assay with flow cytometry. Data shown are mean + SD from three independent experiments.

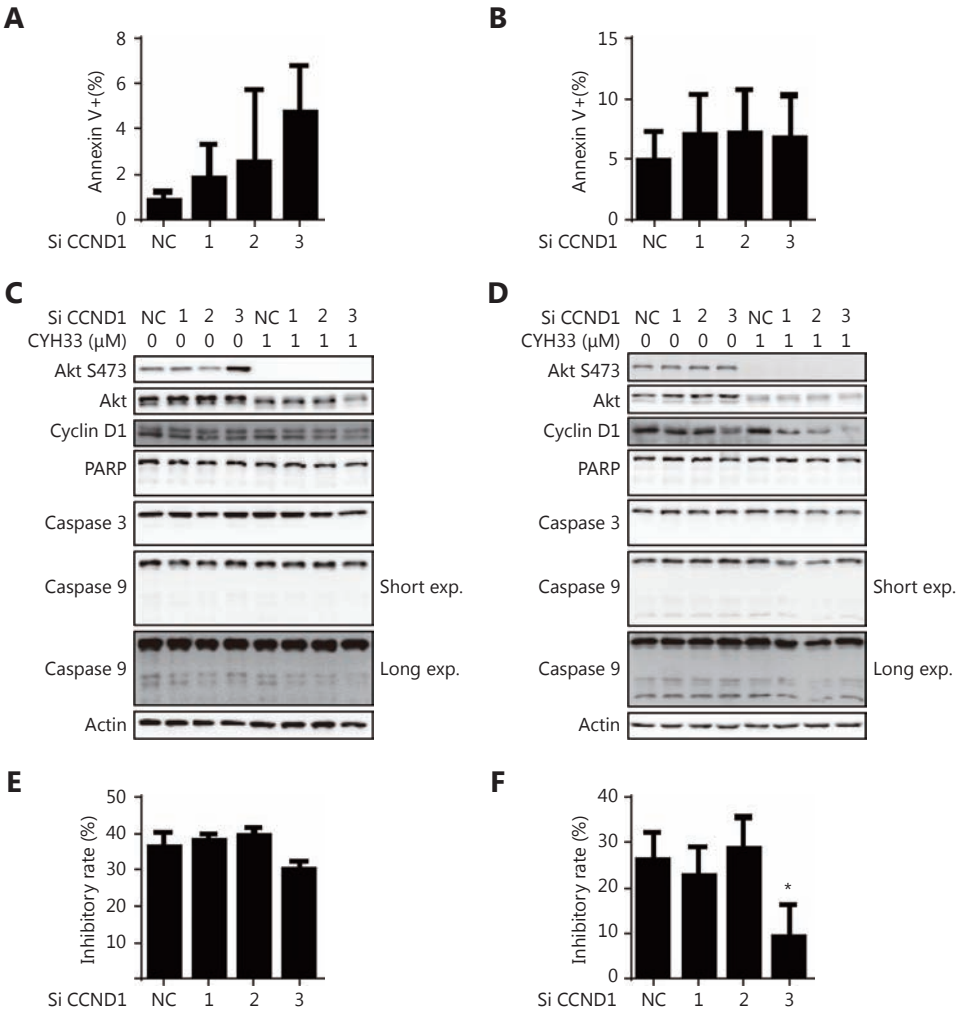

Figure S4 Down-regulation of cyclin D1 had no effect on CYH33-induced apoptosis or the anti-proliferative activity of PD0332991. A549 and H23 cells transfected with siRNAs targeting cyclin D1 or negative control were treated with CYH33 (1 μM) for 72 h (A–D). Induction of apoptosis in A549 (A) and H23 (B) cells was determined by Aneexin-V-PI dual staining. Annexin-V positive cells were measured with flow cytometry. Data shown are mean + SD from three independent experiments. (C–D) Cell lysates of A549 (C) and H23 (D) cells were subjected to Western blot with indicated antibodies. A549 (E) and H23 (F) cells transfected with SiRNA targeting cyclin D1 or negative control were treated with PD0332991 (1 μM) for 72 h, and inhibition of cell proliferation by PD0332991 was calculated. Data shown are mean + SD. Differences between cells transfected with siRNAs targeting cyclin D1 and negative control were analyzed using two-tailed Student's t test. *: $P < 0.05$.

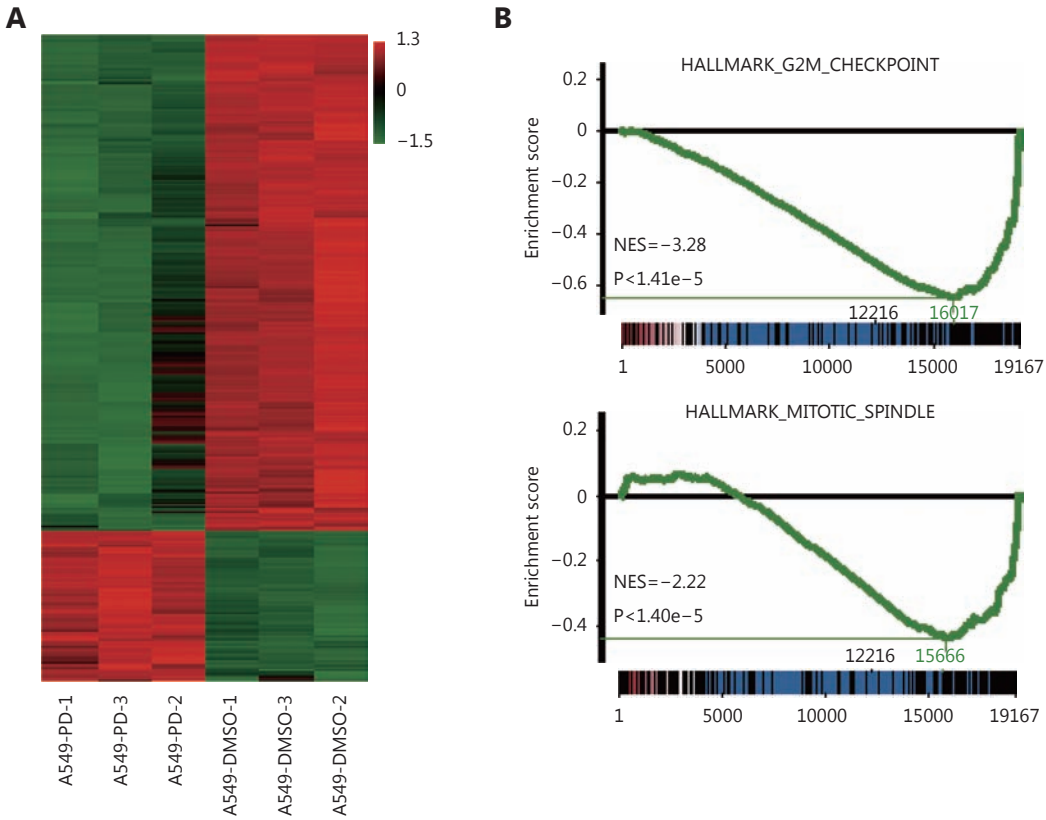

Figure S5 Genome-wide gene expression profiling in A549 cells after PD0332991 treatment. A549 cells were treated with vehicle or PD0332991 (1 μM) for 72 h and total RNA was extracted. Genome-wide gene expression profiling was performed with microarray. (A) The genome-wide gene expression profile of A549 cells treated with vehicle control or PD0332991. Three biological replicates were employed in each group. (B) GSEA enrichment plot of differentially expressed genes in the gene set of hallmark of G2/M checkpoint (HALLMARK_G2/M_Checkpoints) and hallmark of mitotic spindle (HALLMARK_MITOTIC_SPINDLE) upon PD0332991 treatment.

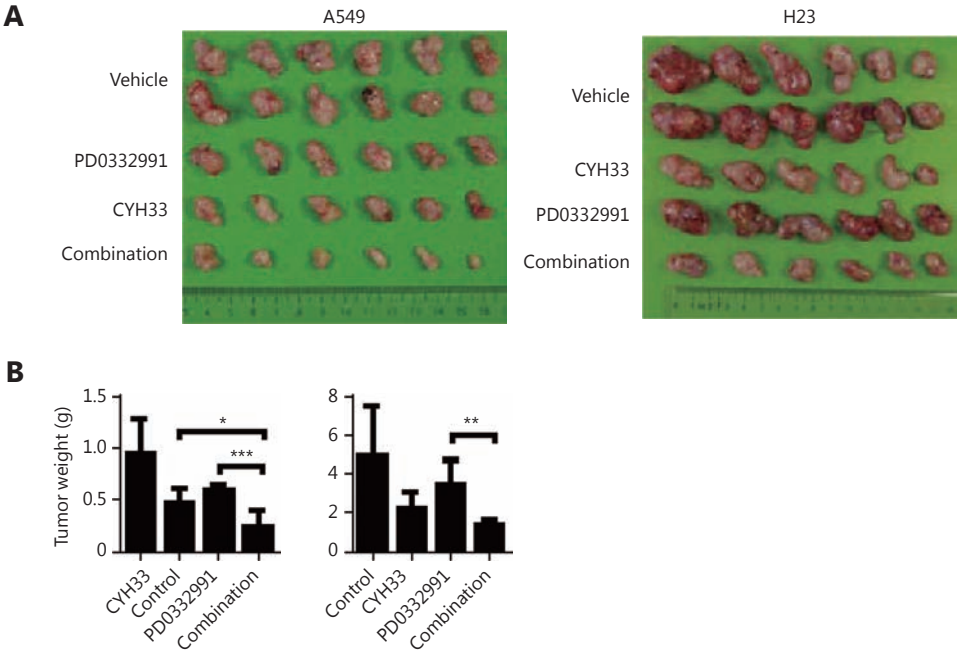

Figure S6 Combined inhibition of PI3Kα and CDK4/6 displays synergistic activity against A549 and H23 xenografts. Randomly grouped nude mice bearing A549 xenografts or H23 xenografts were administrated orally with vehicle control, CYH33, PD0332991 or their combination once a day for 21d (A549) or 14 d (H23). Tumors were collected and weighed at the end of treatment. (A) Image of tumors collected at the end of treatment. (B) Tumor weight of each group was presented as mean + SD. Differences between indicated groups were analyzed using a two-tailed Student's t test. *: $P < 0.05$; **: $P < 0.01$; ***: $P < 0.001$.